@BoneJointRes

Inhibition of PA28γ expression can alleviate osteoarthritis by inhibiting endoplasmic reticulum stress and promoting STAT3 phosphorylation

From Tongji Hospital, Tongji Medical College, Huazhong University of Science and Technology, Wuhan, China

Cite this article:
Bone Joint Res 2024;13(11):
659–672.

DOI: 10.1302/2046-3758.
1311.BJR-2023-0361.R2

Correspondence should be sent to Fengjing Guo
guofjdoc@163.com

H. Mo,[1] K. Sun,[1] Y. Hou,[1] Z. Ruan,[1] Z. He,[1] H. Liu,[1] L. Li,[1,2] Z. Wang,[1] F. Guo[1]

[1]Department of Orthopedics, Tongji Hospital, Tongji Medical College, Huazhong University of Science and Technology, Wuhan, China
[2]Wuhan National High Magnetic Field Center, Huazhong University of Science and Technology, Wuhan, China

Aims

Osteoarthritis (OA) is a common degenerative disease. PA28γ is a member of the 11S proteasome activator and is involved in the regulation of several important cellular processes, including cell proliferation, apoptosis, and inflammation. This study aimed to explore the role of PA28γ in the occurrence and development of OA and its potential mechanism.

Methods

A total of 120 newborn male mice were employed for the isolation and culture of primary chondrocytes. OA-related indicators such as anabolism, catabolism, inflammation, and apoptosis were detected. Effects and related mechanisms of PA28γ in chondrocyte endoplasmic reticulum (ER) stress were studied using western blotting, real-time polymerase chain reaction (PCR), and immunofluorescence. The OA mouse model was established by destabilized medial meniscus (DMM) surgery, and adenovirus was injected into the knee cavity of 15 12-week-old male mice to reduce the expression of PA28γ. The degree of cartilage destruction was evaluated by haematoxylin and eosin (HE) staining, safranin O/fast green staining, toluidine blue staining, and immunohistochemistry.

Results

We found that PA28γ knockdown in chondrocytes can effectively improve anabolism and catabolism and inhibit inflammation, apoptosis, and ER stress. Moreover, PA28γ knockdown affected the phosphorylation of IRE1α and the expression of TRAF2, thereby affecting the mitogen-activated protein kinase (MAPK) and nuclear factor-κB (NF-κB) signalling pathways, and finally affecting the inflammatory response of chondrocytes. In addition, we found that PA28γ knockdown can promote the phosphorylation of signal transducer and activator of transcription 3 (STAT3), thereby inhibiting ER stress in chondrocytes. The use of Stattic (an inhibitor of STAT3 phosphorylation) enhanced ER stress. In vivo, we found that PA28γ knockdown effectively reduced cartilage destruction in a mouse model of OA induced by the DMM surgery.

Conclusion

PA28γ knockdown in chondrocytes can inhibit anabolic and catabolic dysregulation, inflammatory response, and apoptosis in OA. Moreover, PA28γ knockdown in chondrocytes can inhibit ER stress by promoting STAT3 phosphorylation.

Article focus

- In our experiment, we studied the effect of PA28γ in the progression of osteoarthritis (OA) and its potential mechanism in a mouse model.

Bone & Joint Research

Key messages

- PA28γ knockdown in chondrocytes can effectively improve anabolism and catabolism and inhibit inflammation, apoptosis, and endoplasmic reticulum (ER) stress.
- PA28γ knockdown in chondrocytes can inhibit ER stress by promoting STAT3 phosphorylation.

Strengths and limitations

- To our knowledge, we are the first to present evidence that PA28γ is a potential therapeutic target for the treatment of OA.
- The effect of PA28γ overexpression on OA needs to be studied further.

Introduction

Osteoarthritis (OA) is a common degenerative disease in which pain is a very important characteristic and joint mobility disorders may occur, eventually leading to disabilities.[1-3] Owing to the ageing population, the number of patients with OA is also increasing.[1] Compared with that in 1990, the crude incidence of OA increased by 102% in 2017.[4] The progression of OA is accompanied by a series of pathological changes, such as cartilage destruction, osteophyte formation, and synovial inflammation.[3,5-7] OA is closely associated with autophagy, apoptosis, pyroptosis, and ER stress of chondrocytes.[8-10] However, the pathogenesis of OA is still not fully understood, and there is currently no safe and effective treatment for it. Therefore, we need to further explore the molecular mechanisms of OA and identify new therapeutic targets in order to develop more effective treatment strategies.

Endoplasmic reticulum (ER) stress plays a key role in the pathological process of OA.[11,12] Under normal circumstances, ER is involved in important physiological processes such as protein synthesis and transport, protein folding, lipid and steroid synthesis, and maintaining cell homeostasis.[13-15] Under osteoarthritic conditions, misfolded proteins accumulate in large quantities and ER stress is activated.[16] ER stress-related biomarkers, such as glucose regulated protein 78 (GRP78) and C/EBP-homologous protein (CHOP), are up-regulated, and their downstream signalling pathways are further activated, including protein kinase RNA-like ER kinase (PERK), inositol requiring enzyme 1 α (IRE1α), and activating transcription factor 6 (ATF6), ultimately leading to apoptosis and inflammation.[16-19] Therefore, we believe that gene targets capable of alleviating ER stress may be potential therapeutic targets for OA.

PA28γ is a member of the 11S proteasome activator family that binds to and activates the 20S proteasome,[20] thereby regulating several important cellular processes including cell growth and proliferation, apoptosis, autophagy, and responses to DNA damage.[21,22] Recent studies have confirmed that PA28γ is closely related to a variety of inflammatory diseases: PA28γ exacerbates colonic inflammation by activating the NF-κB signalling pathway,[23] and also regulates NF-κB activity by specifically degrading IkBε, thereby regulating inflammation of testicular interstitial cells.[24]

However, the association between PA28γ and OA remains unclear. This was the focus of our study.

Methods

Reagents and antibodies

Recombinant mouse interleukin 1 β (IL-1β) was purchased from PeproTech (USA), and tert-Butyl hydroperoxide (TBHP) was purchased form Sigma-Aldrich (USA). Lipofectamine 3000 reagent was purchased from Invitrogen (Thermo Fisher Scientific, USA). Rabbit anti-glyceraldehyde-3-phosphate dehydrogenase (GAPDH) antibody and primary antibodies against aggrecan, type II collagen (COL2), matrix metalloproteinase-3 (MMP3), and MMP13 were purchased from Proteintech (China). Antibodies against PA28γ, SOX9, iNOS, COX2, BAX, BCL2, clv caspase-3, t caspase-3, CHOP, PERK, p-PERK, TRAF2, JNK, p-JNK, ERK, p-ERK, P38, p-P38, IKKβ, p-IKKαβ, P65, p-P65, and IL-1β were acquired from Cell Signaling Technology (USA). Antibodies against GRP78, IRE1α, p-IREα, STAT3, and p-STAT3 were obtained from Abcam (UK). Anti-rabbit and anti-mouse secondary antibodies for western blot and immunofluorescence analyses, phosphate-buffered saline (PBS) solution, tyrisin, collagenase type II, paraformaldehyde, EDTA, diaminobenzidine, and haematoxylin were acquired from Boster (China).

Isolation and culture of primary chondrocytes

A total of 120 newborn male C57BL/6 mice (seven days old) were euthanized and disinfected. The cartilage was separated from the bilateral knee joints of the mice and cut into three pieces of 1 mm each. Three mice were used to isolate primary chondrocytes each time. This was repeated 40 times in total. Chondrocyte populations from individual animals were maintained as separate biological replicates. Purified cartilage slices were digested with 0.25% trypsin at 37°C for 20 minutes and then digested with 0.2% collagenase II at 37°C for eight hours. After suspension and filtration, the released chondrocytes were cultured in Dulbecco's Modified Eagle Medium (DMEM)/F12 (supplemented with 10% fetal bovine serum, 1% streptomycin sulphate, and 1% penicillin) at 37°C, and the medium was changed every two days. Before each experiment, first- or second-generation cells were laid out on 10 cm plates. In each experiment, including negative or positive controls, chondrocytes were cultured for five days to achieve approximately 70% to 80% density and 70% confluence.

siRNA transfection

According to the manufacturer's instructions (Ribbio, China), PA28γ-targeting small interfering RNA (siRNA) and Lipofectamine 3000 transfection reagents were mixed with Opti-MEM culture media, and the mixture was then added to the chondrocyte culture medium. The siRNA concentration was 50 nM. PA28γ-targeting siRNA had the following sense chain: 5´-CAGAAGACUUGGUGGCAAATT-3´. Similarly, non-targeting control siRNA and Lipofectamine 3000 transfection reagents were mixed with Opti-MEM culture media, and the mixture was then added to the chondrocyte culture medium. The siRNA concentration was 50 nM.

RNA extraction and RT-qPCR

RNA was extracted from chondrocytes using the OMEGA kit (Omega Bio-tek, USA). A Revert Aid First Strand cDNA Synthesis Kit (Yeasen, China) was used to synthesize cDNA. The SYBR Green Quantitative PCR protocol was used to amplify

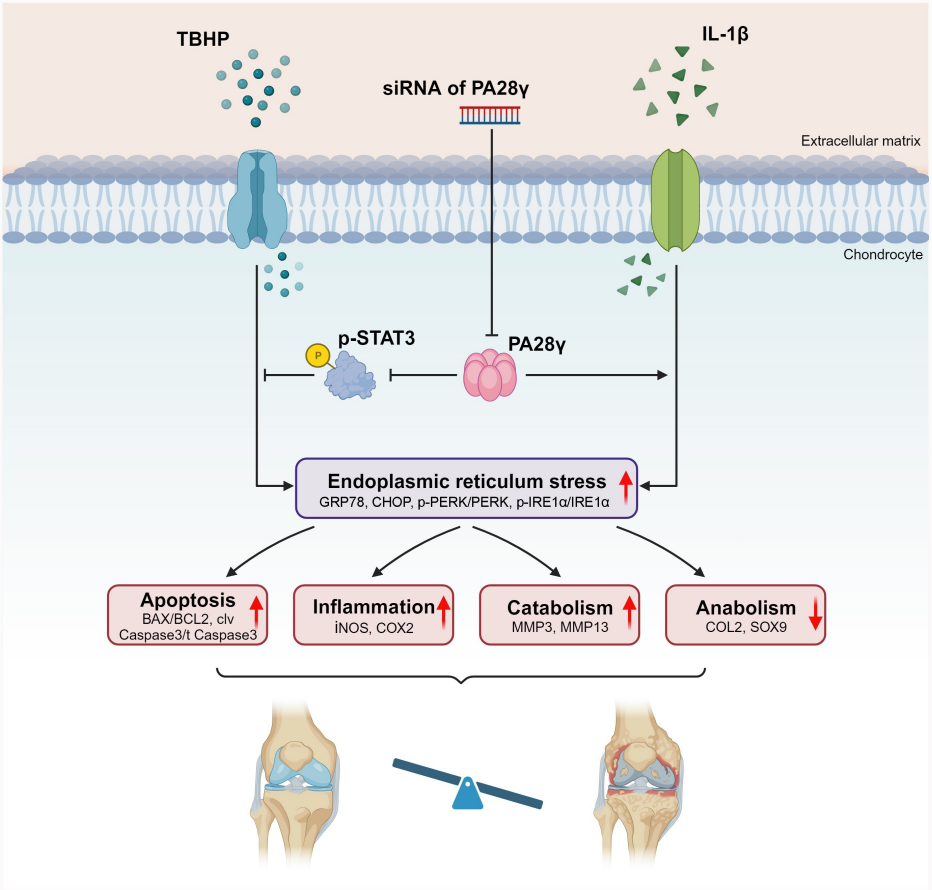

Fig. 1
Schematic illustration of effect of PA28γ knockdown in osteoarthritis development (figure was created with BioRender.com). BAX, Bcl-2 Associated X-protein; COL2, type II collagen; COX2, cyclooxygenase-2; GRP78, Glucose-Regulated Protein 78; IL-1, interleukin-1β; iNOS, inducible nitric oxide synthase; IRE1α, inositol-requiring enzyme type 1 alpha; MMP, matrix metalloproteinase; PA28γ, proteasome activator 28γ; PERK, protein kinase-like endoplasmic reticulum kinase; SOX9, SRY-Box Transcription Factor 9; STAT3, signal transducer and activator of transcription 3; TBHP, tert-butylhydrogen peroxide.

the template to determine the messenger RNA levels. Primer sequences are described in Table I.

Expression levels of target genes were calculated using the 2−ΔΔCq method.

Western blotting analysis

Cultured chondrocytes were lysed for 30 minutes in ice-cold RIPA lysis buffer (Boster) containing 1% protease and phosphatase inhibitors (Boster); protease and phosphatase inhibitors can protect proteins during the preparation of cell lysates. The cell lysates were then immediately centrifuged at 10,000 ×g at 4°C for 30 minutes. Equal amounts of protein were loaded onto SDS-PAGE gels (10% to 15%) for electrophoresis. After electrophoresis, the proteins were transferred from the gels onto polyvinylidene fluoride membranes. Each membrane was blocked with 5% non-fat milk in Tris-buffered saline containing 0.1% Tween 20 buffer for one hour and then incubated with primary antibodies, including COL2 (dilution 1: 800), MMP3 (dilution 1: 800), MMP13 (dilution 1: 800), PA28γ (dilution 1: 1,000), SOX9 (dilution 1: 1,000), iNOS (dilution 1: 1,000), COX2 (dilution 1: 1,000), BAX (dilution 1: 1,000), BCL2 (dilution 1: 1,000), clv caspase-3 (dilution 1: 1,000), t caspase-3 (dilution 1: 1,000), CHOP (dilution 1: 1,000), PERK (dilution 1: 1,000), p-PERK (dilution 1: 1,000), GRP78 (dilution 1: 1,000), IRE1α (dilution 1: 1,000), p-IREα (dilution 1: 1,000), TRAF2 (dilution 1: 1,000), JNK (dilution 1: 1,000), p-JNK (dilution 1: 1,000), ERK (dilution 1: 1,000), p-ERK (dilution 1: 1,000), P38 (dilution 1: 1,000), p-P38 (dilution 1: 1,000), IKKβ (dilution 1: 1,000), p-IKKαβ (dilution 1: 1,000), P65 (dilution 1: 1,000), p-P65 (dilution 1: 1,000), STAT3 (dilution 1: 1,000), and p-STAT3 (dilution 1: 1,000) overnight at 4°C on a shaker. After incubation with horseradish peroxidase-conjugated secondary antibodies for one hour, proteins were visualized using an enhanced chemiluminescence kit (Thermo Fisher Scientific, USA) in a ChemiDoc XRS System (Bio-Rad Laboratories, USA). Proteins were quantified using Image Lab software (Bio-Rad Laboratories, USA), and the target protein levels were normalized to GAPDH or relative total protein levels.

Immunofluorescence

COX2 and CHOP in chondrocytes was analyzed by immunofluorescence staining. After fixation in 4% paraformaldehyde and permeation in 0.2% Triton X-100, chondrocytes were incubated overnight with a primary antibody for COX2 and CHOP (1:100) at 4°C. The cells were then incubated with anti-mouse and anti-rabbit secondary antibodies for one hour. Finally, images were captured using a fluorescence microscope.

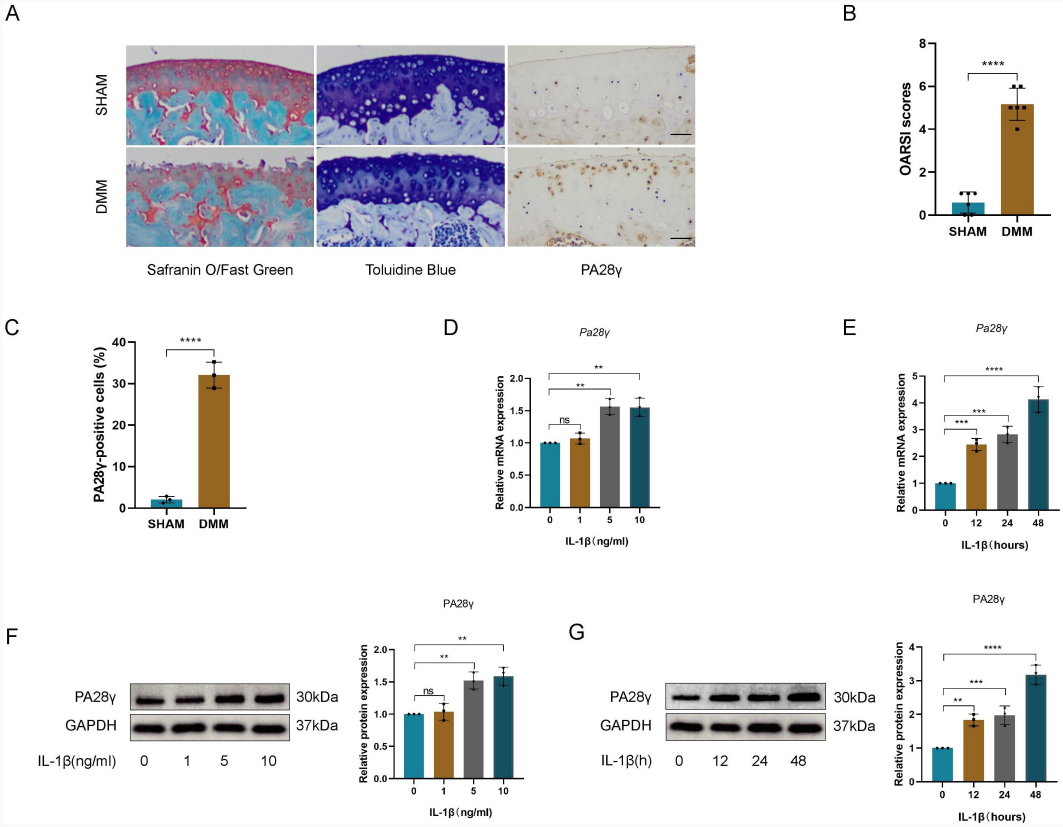

Fig. 2

PA28γ expression increased in both in vitro and in vivo models of osteoarthritis (OA). a) Representative safranin O/solid green staining images, toluidine blue staining images, and immunohistochemical images of PA28γ in articular cartilage of destabilized medial meniscus (DMM) and sham mice, measuring scale = 100 μm, magnification: ×200. b) Osteoarthritis Research Society International (OARSI) score of DMM and sham mice (n = 6, ****p < 0.0001). c) Quantitative analysis of PA28γ-positive chondrocyte in cartilage from DMM and sham mice (n = 3, ****p < 0.0001). d) PA28γ mRNA levels were measured by quantitative real-time polymerase chain reaction (qRT-PCR) after chondrocytes were stimulated with various concentrations of interleukin-1β (IL-1β) for 48 hours (**p < 0.01). e) PA28γ mRNA levels were measured by qRT-PCR after chondrocytes were stimulated with 5 ng/ml IL-1β for different durations (***p < 0.001, ****p < 0.0001). f) Western blotting and quantitative data of PA28γ expression 48 hours obtained after stimulating chondrocytes with various concentrations of IL-1β (**p < 0.01). g) PA28γ representative western blotting and quantitative data obtained after stimulating chondrocytes with 5 ng/ml IL-1β for different durations (**p < 0.01, ***p < 0.001, ****p < 0.0001).

Cellular safranin O staining

Primary chondrocytes were seeded in 24-well culture plates and stimulated with siRNA and IL-1β for 48 hours. Next, chondrocytes were washed with PBS three times to remove the culture medium and fixed with 4% paraformaldehyde for 20 minutes at room temperature. After washing with PBS again, staining was performed with safranin O working solution (Bobst, China) for one hour at 37°C. The remaining safranin O working solution was removed and chondrocytes were washed three times with PBS. Finally, an inverted light microscope (Bio-Rad Laboratories) was used to observe the results.[25]

Cellular toluidine blue staining

Primary chondrocytes were seeded in 24-well culture plates and stimulated with siRNA and IL-1β for 48 hours. Next, chondrocytes were washed with PBS three times to remove the culture medium and fixed with 4% paraformaldehyde for 20 minutes at room temperature. After washing with PBS again, staining was performed with toluidine blue working solution (Bobst) for four hours at 37°C. The remaining dye was removed and chondrocytes were washed three times with PBS. Finally, an inverted light microscope was used to observe the results.[25]

Flow cytometry

Annexin V-FITC apoptosis detection kit (Yeasen, China) was used to identify the cell apoptosis rate. Chondrocytes were digested by trypsin without ethylenediaminetetraacetic acid (EDTA). Annexin V-FITC (5 μl) and propidium iodide (PI) (10 μl) were added to the flow tube under dark conditions, mixed, and kept to react for 15 to 30 minutes. The results were analyzed by flow cytometry. Forward scatter (FSC) and side scatter (SSC) are indicators of cell size, cell granularity, and complexity. Chondrocyte populations were determined in the FSC > 3 × 10^5 and SSC > 3 × 10^5 ranges. Apoptosis was measured using Annexin V and PI as probes. Annexin-negative and PI-negative cells were regarded as live cells; annexin-positive and PI-negative cells were considered as early apoptotic cells; and annexin-positive and PI-positive cells represented late-stage apoptotic cells.

Animal models

Our animal study adhered to the ARRIVE checklist. Experiments were approved by our Animal Laboratory Ethics

Table I. Primer sequences.

Gene	Sequence
PA28γ	5′ -ACAAGTGAGGCAGAAGAC-3′ , 5′ -ATCATGGCTATTG GTGAG-3′
COL2	5'-GGCCAGGATGCCCGAAAATTA-3', 5'-CGCACCCT TTTCTCC CTTGT-3'
SOX9	5′ -AGGAAGTCGGTGAAGAACGG-3′ , 5′ -GGACCCTG AG ATTGCCCAGA-3′
MMP3	5′ -ACTCCCTGGGACTCTACCAC-3′ , 5′ -GGTACCAC GAG GACATCAGG-3′
MMP13	5′ -TGATGGACCTTCTGGTCTTCTGG-3′ , 5′ -CATCC ACAT GGTTGGGAAGTTCT-3′
iNOS	5′ -GACCCAGAGACAAGCCT AC-3′ , 5′ -GTGAGCTGGTAG GTTCCTG-3′
IL-6	5′ -CAACGATGATGCACTTGCAGA-3′ , 5′ -TGTGACTCCAG CTTATCTCTTGG-3′
TNF-α	5′ -CTCAGCGAGGACAGCAAGG-3′ , 5′ -CTCAGCGAGGA CAGCAAGG-3′

COL2, type II collagen; IL-6, interleukin 6; iNOS, inducible nitric oxide synthase; MMP, matrix metalloproteinase; PA28γ, proteasome activator 28γ; SOX9, SRY-box transcription factor 9; TNF-α, tumour necrosis factor α.

Committee. OA was induced in 12-week-old male C57BL/6J mice by destabilized medial meniscus (DMM) surgery. In this experiment, 60 mice were divided into four groups: 1) Sham operation group, in which sham operated mice were administered AD-SHcontrol adenovirus (n = 15); 2) Sham operation + AD-SHPA28γ group, in which sham operated mice were administered AD-SHPA28γ adenovirus (n = 15); 3) DMM group, in which mice that underwent DMM surgery were administered AD-SHcontrol adenovirus (n = 15); and 4) DMM + AD-SHPA28γ group, in which mice that underwent DMM surgery were administered AD-SHPA28γ adenovirus (n = 15). After anaesthesia, the medial meniscus-tibial ligament was severed in the experimental group. In the control group, sham surgery was performed to remove only the fat pad beneath the patella. One week after the DMM and sham surgeries were done, the granulation tissue almost filled up the damaged area, the wound epithelium was epithelialized, and the wound was basically healed. One week after the DMM and sham surgeries were done, mice were injected intra-articularly with 10 µl AD-SHPA28γ or AD-negative adenovirus (1×10^9 plaque-formation units (PFUs)) twice a week for eight weeks.

Histopathological and immunocytochemical analysis

Eight weeks after intra-articular injection, the right knee joints of all mice were dissected. After immersion in 4% paraformaldehyde for 24 hours, the knee joints were transferred to a reagent containing 10% EDTA for decalcification for 30 days. Next, these decalcified samples were embedded in paraffin and cut into 5 µm sections for further tissue staining analysis, which included haematoxylin-eosin (HE), safranin O/fast green, and toluidine blue staining. Immunohistological analyses were performed using antibodies against PA28γ (dilution 1: 100), Aggrecan (dilution 1: 200), COL2 (dilution 1: 200), SOX9 (dilution 1: 200), MMP3 (dilution 1: 100), MMP13 (dilution 1: 100), IL-1β (dilution 1: 200), COX2 (dilution 1: 100), and CHOP (dilution 1: 100). Samples required deparaffinization, rehydration, and blocking, and were stained with diaminobenzidine and counterstained with haematoxylin. Osteoarthritis Research Society International (OARSI) scoring system was applied to evaluate severity of cartilage degeneration in medial tibial plateau and femoral condyle on the sagittal plane. Each knee joint was scored six times and averaged.

Statistical analysis

All in vitro experiments were repeated in triplicate. The results were analyzed using GraphPad Prism V.8.4.0 software (GraphPad, USA). Data are shown as the mean (SD) and were analyzed using one-way analysis of variance (ANOVA). Non-parametric data (OARSI scores) were analyzed using the Kruskal-Wallis H test. Statistical significance was defined as $p < 0.05$. The analysis of western blotting and PCR results is relative expression. In the results of western blotting and PCR, we regarded the first group as the reference group.

Results

PA28γ expression increased in both in vitro and in vivo models of OA

To investigate the role of PA28γ in the destruction of knee cartilage, we evaluated the expression of PA28γ in the knee cartilage of OA mice (Figure 1). Safranin O/solid green staining, toluidine blue staining, and OARSI score showed obvious cartilage destruction in knee joint of mice in the DMM group (Figures 2a and 2b). Immunohistochemically, the expression of PA28γ in knee cartilage of mice in the DMM group was significantly higher than that of mice in the sham group (Figures 2a and 2c). Next, primary mouse chondrocytes were treated with different concentrations of IL-1β (0, 1, 5, and 10 ng/ml) for 48 hours. No statistically significant change was observed at 1 ng/ml; however, PA28γ expression was significantly increased at 5 and 10 ng/ml (Figures 2d and 2f). Further, primary mouse chondrocytes were treated with IL-1β at a concentration of 5 ng/ml for 0, 12, 24, and 48 hours. At 12 and 24 hours, PA28γ expression increased significantly, and the increase was even more significant at 48 hours (Figures 2e and 2g). In conclusion, our data showed that PA28γ expression increased in both in vitro and in vivo models of OA.

Knockdown of PA28γ alleviates IL-1β-induced dysregulation of anabolism and catabolism in chondrocytes

During the pathogenesis of OA, the expression of proteins involved in anabolism, such as COL2 (a structural protein) and SOX9 (a transcription factor), decreases, whereas the expression of proteins involved in catabolism, such as MMP3 and MMP13, increases.[26,27] In our study, the knockdown efficiency of PA28γ was detected after transfection of chondrocytes with small interfering negative control (si-NC) or si-PA28γ for 48 hours, and the results showed that the expression of PA28γ in chondrocytes was significantly inhibited (Figures 3a and 3b). Next, we stimulated chondrocytes with IL-1β, which reduced mRNA and protein expression of COL2 and SOX9, while these decreases were attenuated by PA28γ knockdown (Figures 3c and 3e). Similarly, IL-1β increased mRNA and protein expression of MMP3 and MMP13, while PA28γ knockdown partially reversed these changes (Figures 3d and 3f). Safranin O and

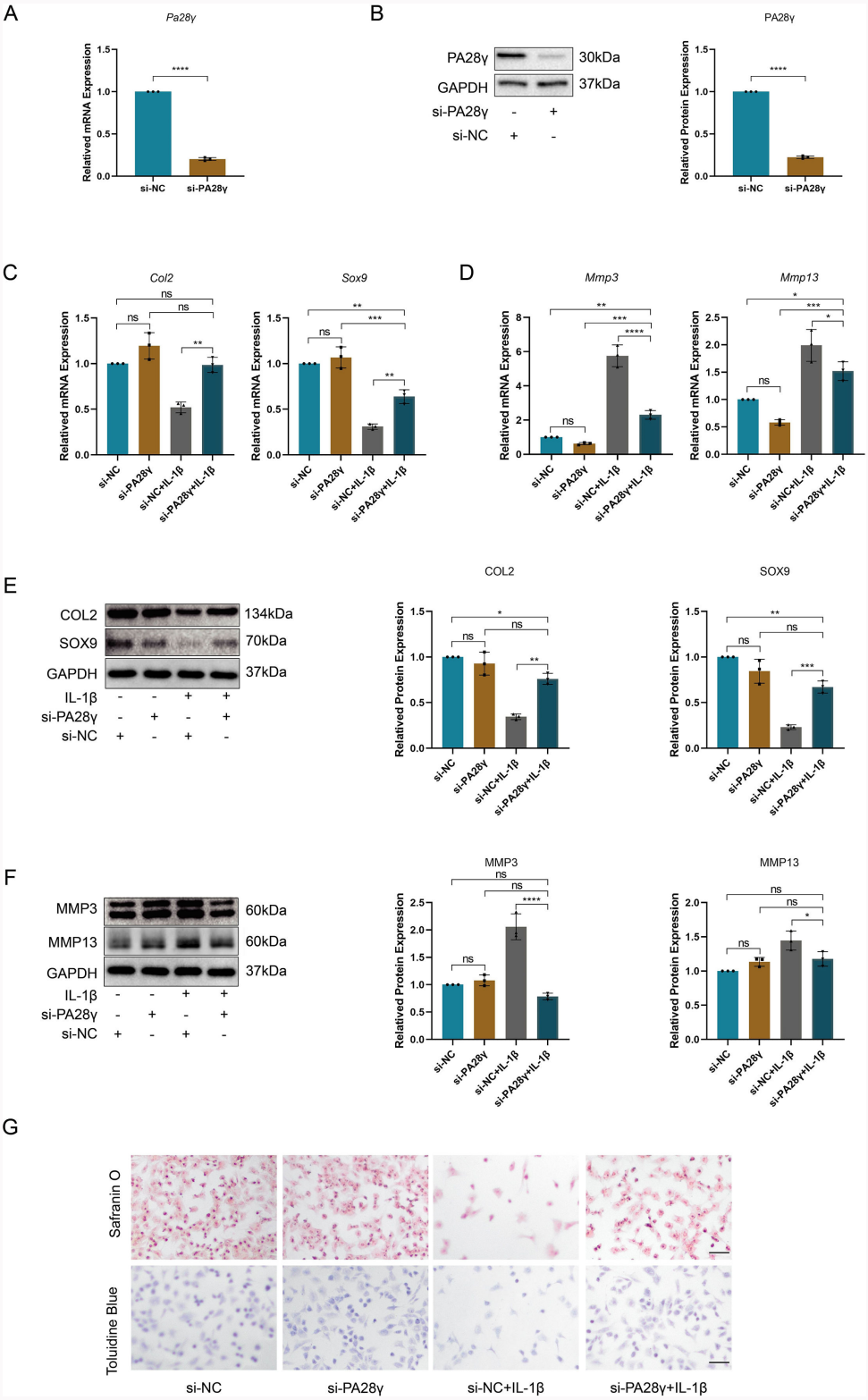

Fig. 3

Knockdown of PA28γ alleviates interleukin-1β (IL-1β)-induced dysregulation of anabolism and catabolism in chondrocytes. a) After transfection of chondrocytes with si-NC or si-PA28γ for 24 hrs, the knockdown efficiency of PA28γ was detected by quantitative real-time polymerase chain reaction (qRT-PCR) (****p < 0.0001). b) After transfection of chondrocytes with si-NC or si-PA28γ for 24 hrs, the knockdown efficiency of PA28γ was detected by western blotting (****p < 0.0001). c) mRNA expression of type II collagen (COL2) and SOX9 after transfection of chondrocytes with si-NC or si-PA28γ and treatment with IL-1β (**p < 0.01, ***p < 0.001). d) mRNA expression of matrix metalloproteinase-3 (MMP3) and MMP13 after transfection of chondrocytes with si-NC or si-PA28γ and treatment with IL-1β (*p < 0.05, **p < 0.01, ***p < 0.001, ****p < 0.0001). e) Representative western blotting and quantitative data of COL2 and SOX9 after transfection of chondrocytes with si-NC or si-PA28γ and treatment with IL-1β (*p < 0.05, **p < 0.01, ***p < 0.001). f) Representative western blotting and quantitative data of MMP3 and MMP13 after transfection of chondrocytes with si-NC or si-PA28γ and treatment with IL-1β (*p < 0.05, ****p < 0.0001). g) Safranin O and toluidine blue staining image after transfection of chondrocytes with si-NC or si-PA28γ and treatment with IL-1β, measuring scale = 100 μm, magnification: ×200.

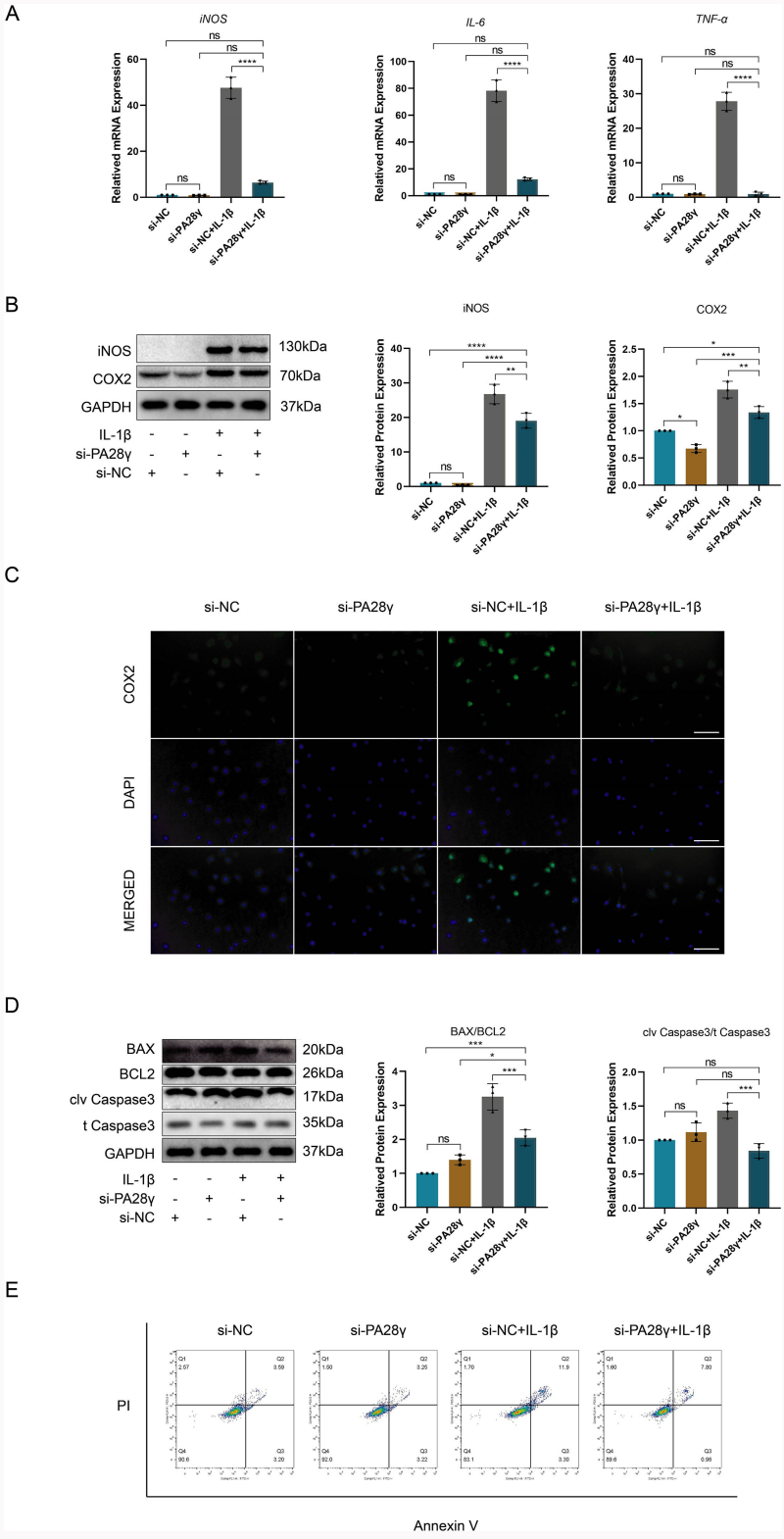

Fig. 4

Knockdown of PA28γ alleviates interleukin-1β (IL-1β)-induced inflammation and apoptosis in chondrocytes. a) mRNA expression of iNOS, IL-6, and tumour necrosis factor-α (TNF-α) after transfection of chondrocytes with si-NC or si-PA28γ and treatment with IL-1β (****p < 0.0001). b) Representative western blotting and quantitative data of iNOS and COX2 after transfection of chondrocytes with si-NC or si-PA28γ and treatment with IL-1β (*p < 0.05, **p < 0.01, ***p < 0.001, ****p < 0.0001). c) COX2 representative immunofluorescence images of chondrocytes transfected with si-NC or si-PA28γ and treated with IL-1β, measuring scale = 100 μm. d) Representative western blotting and quantitative data of BAX, BCL2, clv Caspase3, and t Caspase3 after transfection of chondrocytes with si-NC or si-PA28γ and treatment with IL-1β (*p < 0.05, ***p < 0.001). e) Flow cytometry with annexin V-FITC/PI apoptosis analysis after transfection of chondrocytes with si-NC or si-PA28γ and treatment with IL-1β. DAPI, 4′,6-diamidino-2-phenylindole; GAPDH, glyceraldehyde-3-phosphate dehydrogenase; ns, not significant.

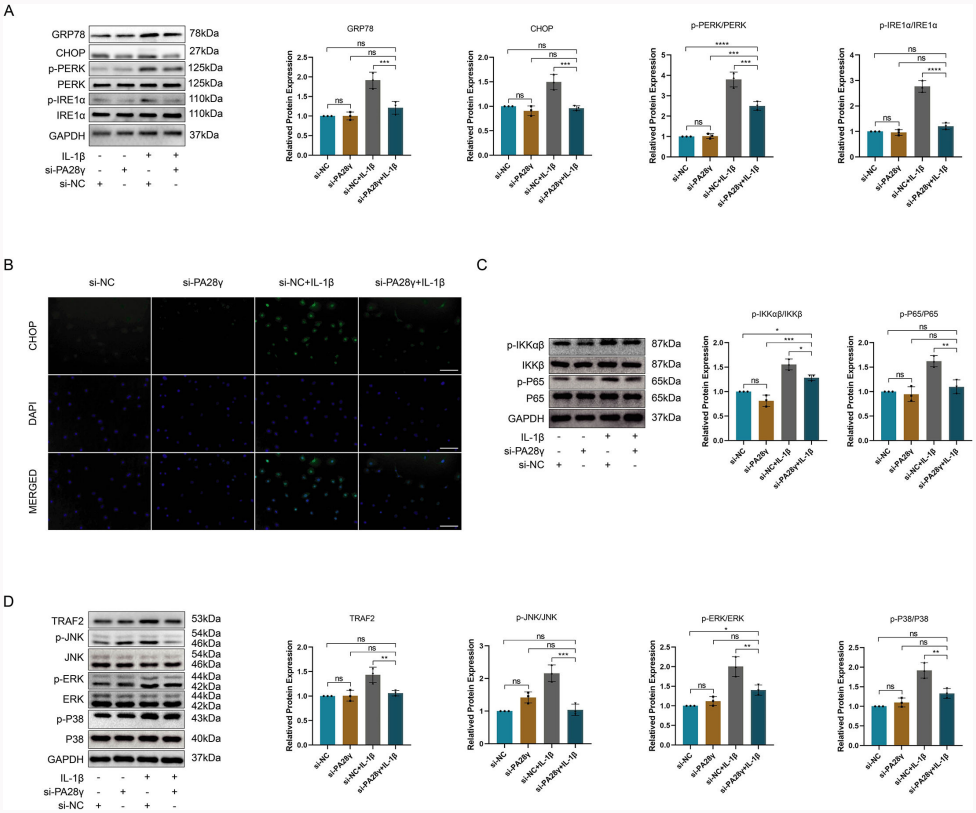

Fig. 5

Knockdown of PA28γ alleviates interleukin-1β (IL-1β)-induced endoplasmic reticulum (ER) stress in chondrocytes. a) Representative western blotting and quantitative data of GRP78, CHOP, PERK, p-PERK, IRE1α, and p-IRE1α after transfection of chondrocytes with si-NC or si-PA28γ and treatment with IL-1β (***p < 0.001, ****p < 0.0001). b) CHOP representative immunofluorescence images of chondrocytes transfected with si-NC or si-PA28γ and treated with IL-1β, measuring scale = 100 μm. c) Representative western blotting and quantitative data of IKKβ, p-IKKαβ, P65, and p-P65 after transfection of chondrocytes with si-NC or si-PA28γ and treatment with IL-1β (*p < 0.05, **p < 0.01, ***p < 0.001). d) Representative western blotting and quantitative data of tumour necrosis factor receptor-associated factor 2 (TRAF2), JNK, p-JNK, ERK, p-ERK, P38, and p-P38 after transfection of chondrocytes with si-NC or si-PA28γ and treatment with IL-1β (*p < 0.05, **p < 0.01, ***p < 0.001). DAPI, 4′,6-diamidino-2-phenylindole; GAPDH, glyceraldehyde-3-phosphate dehydrogenase; ns, not significant.

toluidine blue staining showed that IL-1β reduced the density and staining intensity of chondrocytes, reflecting the decrease of proteoglycan content in chondrocytes. These changes were reversed to some extent after PA28γ was knocked down (Figure 3g).

Knockdown of PA28γ alleviates IL-1β-induced inflammation and apoptosis in chondrocytes

In order to further investigate the effect of PA28γ on chondrocyte inflammation, chondrocytes were stimulated with IL-1β. The results showed that the mRNA expressions of iNOS, IL-6, and TNF-α were increased after IL-1β treatment of chondrocytes. PA28γ knockdown decreased the mRNA expression of iNOS, IL-6, and TNF-α (Figure 4a). Western blotting further demonstrated that PA28γ knockdown decreased the protein expression of iNOS and COX2 after IL-1β treatment of chondrocytes (Figure 4b). Immunofluorescence also showed that PA28γ knockdown decreased the fluorescence intensity of COX2 after IL-1β treatment of chondrocytes (Figure 4c). One previous study showed that IL-1β can induce apoptosis of chondrocytes.[28] Our results show that transfecting si-PA28γ in chondrocytes can inhibit IL-1β-induced apoptosis to a significant degree ($p < 0.05$). Western blotting showed that knocking down PA28γ inhibited the ratio of IL-1β-stimulated BAX/BCL2 and clv Caspase3/t Caspase3 (Figure 4d). Flow cytometry showed the original results of the apoptosis rate of chondrocytes, and the results showed that IL-1β can promote apoptosis of chondrocytes and increase Annexin-positive cells. PA28γ knockdown reversed this change to some extent and Annexin-positive cells decreased (Figure 4e).

Knockdown of PA28γ alleviates IL-1β-induced ER stress in chondrocytes

Knockdown of PA28γ alleviates IL-1β-induced inflammation and apoptosis in chondrocytes. To investigate whether ER stress is related to these effects, ER stress markers GRP78 and CHOP were evaluated by western blot. Results showed that the protein expression of GRP78 and CHOP was increased after IL-1β treatment of chondrocytes, and PA28γ knockdown attenuated the IL-1β-induced protein expression increase of GRP78 and CHOP (Figure 5a). In addition, we demonstrated that PA28γ down-regulation can affect the phosphorylation of PERK and IRE1α, important targets in the ER stress signalling pathway (Figure 5a). Immunofluorescence also showed that PA28γ knockdown decreased the fluorescence intensity of CHOP after IL-1β treatment of chondrocytes (Figure 5b). Many studies have shown that after ER stress activation, IRE1α recruits TNF receptor-associated factor 2 (TRAF2) to the ER membrane to initiate inflammatory responses via the nuclear factor kappa B (NF-κB) and mitogen-activated protein

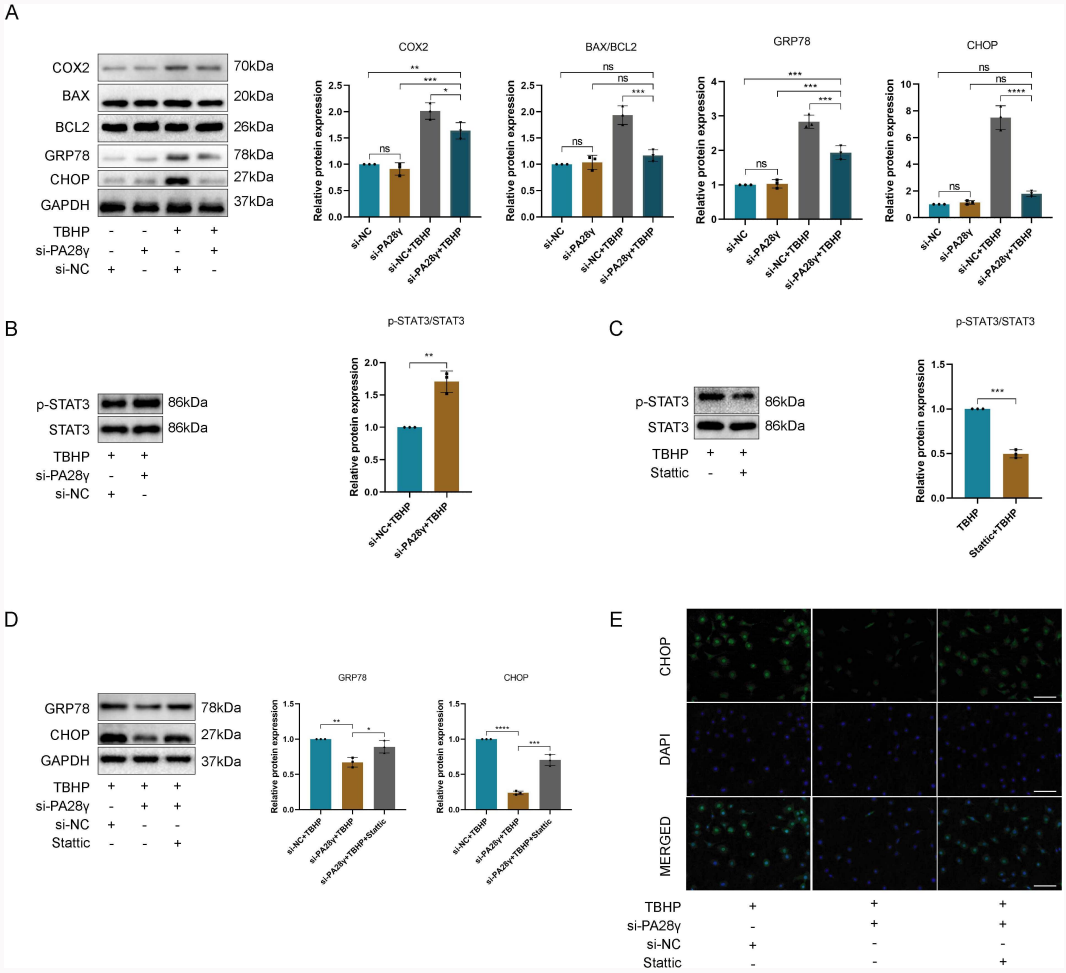

Fig. 6

PA28γ knockdown inhibits endoplasmic reticulum (ER) stress in chondrocytes by promoting signal transducer and activator of transcription 3 (STAT3) phosphorylation. a) Representative western blotting and quantitative data of COX2, BAX, BCL2, GRP78, and CHOP after transfection of chondrocytes with si-NC or si-PA28γ and treatment with tert-butylhydrogen peroxide (TBHP) (*p < 0.05, **p < 0.01, ***p < 0.001, ****p < 0.0001). b) Representative western blotting and quantitative data of STAT3 and p STAT3 after transfection of chondrocytes with si-NC or si-PA28γ and treatment with TBHP, **p < 0.01. c) Representative western blotting and quantitative data of STAT3 and p-STAT3 after treatment with TBHP and Stattic (***p < 0.001). d) Representative western blotting and quantitative data of GRP78 and CHOP after transfection of chondrocytes with si-NC or si-PA28γ and treatment with TBHP and Stattic (*p < 0.05, **p < 0.01, ***p < 0.001, ****p < 0.0001). e) CHOP representative immunofluorescence images of chondrocytes transfected with si-NC or si-PA28γ and treated with TBHP and Stattic, measuring scale = 100 μm, magnification: ×200. DAPI, 4′,6-diamidino-2-phenylindole; GAPDH, glyceraldehyde-3-phosphate dehydrogenase; ns, not significant.

kinases (MAPK) pathway.[29,30] Our study has shown that PA28γ knockdown affects the phosphorylation of IRE1α and the expression of TRAF2, thereby affecting the MAPK and NF-κB signalling pathways, and finally affecting the inflammatory response of chondrocytes (Figures 5c and 5d).

Knockdown of PA28γ inhibits ER stress in chondrocytes by promoting STAT3 phosphorylation

We further explored the mechanism by which PA28γ knockdown affects ER stress in chondrocytes. Since tert-butylhydrogen peroxide (TBHP) is a common inducer of ER stress, and the use of TBHP in OA studies has been reported in several studies,[9,19] we chose this compound to induce ER stress in chondrocytes in our study. The results showed that after TBHP treatment of chondrocytes, the protein expressions of COX2, BAX, GRP78, and CHOP were increased, while the protein expression of BCL2 was decreased. After PA28γ was knocked down, the above changes were inhibited to a certain extent (Figure 6a). STAT3 plays a key role in ER stress, and its phosphorylation is elevated after PA28γ is knocked down in TBHP-treated chondrocytes (Figure 6b). After treatment of chondrocytes with Stattic (a phosphorylation inhibitor of STAT3), the phosphorylation of STAT3 was decreased (Figure 6c). Finally, the results showed that protein expression of GRP78 and CHOP decreased after PA28γ was knocked down in TBHP-treated chondrocytes, while protein expression of GRP78 and CHOP increased after Stattic treatment (Figure 6d). Immunofluorescence staining of CHOP showed similar experimental results (Figure 6e). In summary, our results show that PA28γ knockdown inhibits ER stress in chondrocytes by promoting STAT3 phosphorylation.

Knockdown of PA28γ alleviates OA after DMM surgery

To explore the possible association between PA28γ and OA in vivo, a mouse OA model was induced by destabilized medial meniscus (DMM) surgery. In the sham surgery group and the DMM group, mice were given weekly intra-articular injections of Ad-shControl or Ad-shPA28γ

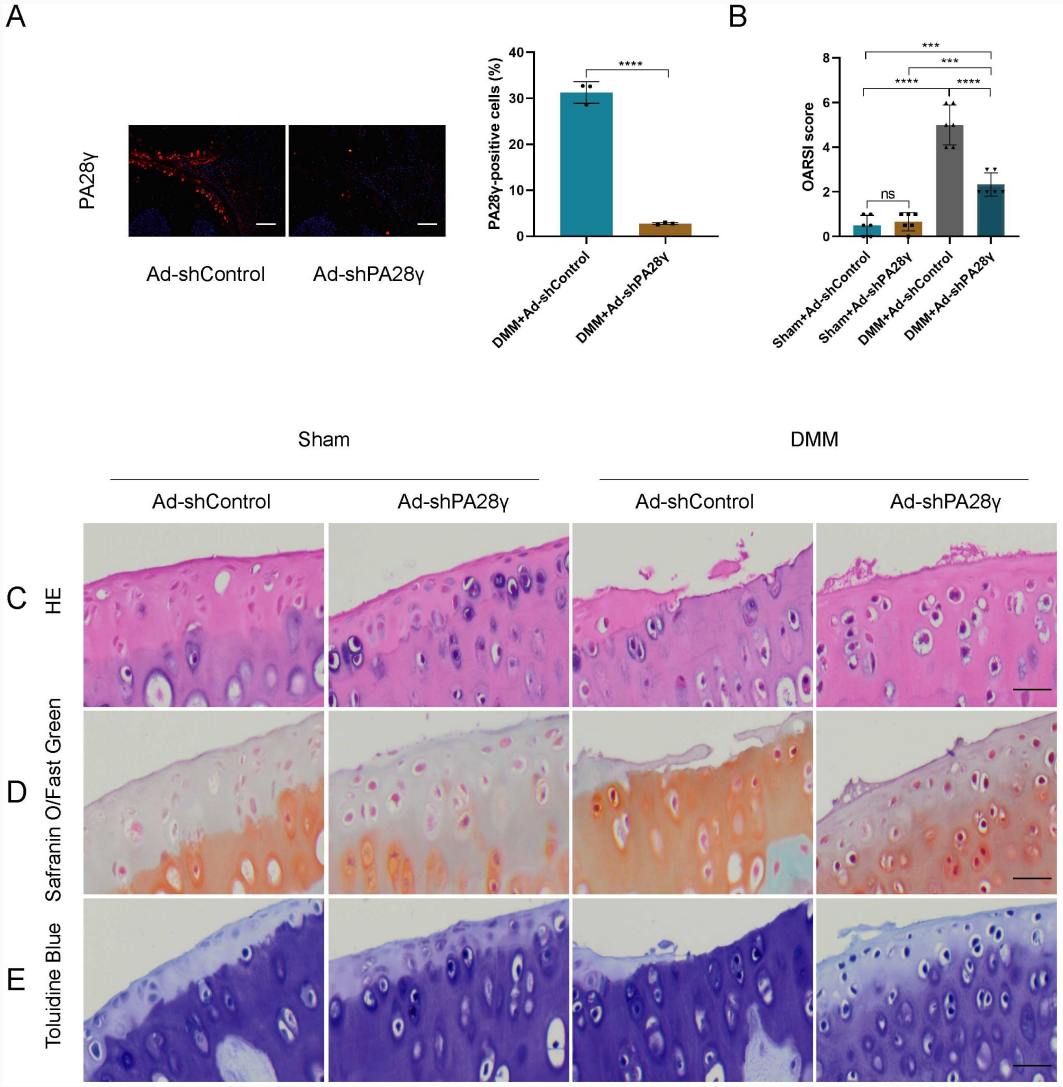

Fig. 7

Knockdown of PA28γ alleviates osteoarthritis (OA) after destabilized medial meniscus (DMM) surgery. a) PA28γ representative immunofluorescence staining images and quantitative data of knee joint tissue obtained from Ad-shControl and Ad-shPA28γ mice eight weeks after DMM surgery, measuring scale = 100 μm, magnification: ×200 (n = 3, ****p < 0.0001). b) Osteoarthritis Research Society International (OARSI) score of mouse knee joint (n = 6, ***p < 0.001, ****p < 0.0001). c) Haematoxylin and eosin (HE) staining images of knee joint tissue obtained from Ad-shControl and Ad-shPA28γ mice eight weeks after DMM surgery, measuring scale = 100 μm. d) Safranin O/solid green staining images of knee joint tissue obtained from Ad-shControl and Ad-shPA28γ mice eight weeks after DMM surgery, measuring scale = 100 μm. e) Toluidine blue staining images of knee joint tissue obtained from Ad-shControl and Ad-shPA28γ mice eight weeks after DMM surgery, measuring scale = 100 μm, magnification: ×400.

adenovirus. Immunofluorescence, HE, safranin O/solid green, toluidine blue, and immunohistochemical staining were performed eight weeks after surgery. The results showed that adenovirus could effectively inhibit the expression of PA28γ in knee cartilage (Figure 7a). Compared with the sham operation group, the DMM group found that the joint cartilage was significantly damaged, proteoglycan was lost, and OARSI score was increased. However, when we reduced the expression of PA28γ, these changes were inhibited to a certain extent (Figures 7b to 7e). Immunohistochemical staining showed that anabolic-related proteins (aggrecan, COL2, and SOX9) were decreased in the DMM group, and the decreases of aggrecan, COL2, and SOX9 were inhibited after the expression of PA28γ was decreased (Figures 8a to 8c, and 8i to 8k). Catabolic-related proteins (MMP3 and MMP13) were increased in the DMM group, and the increases of MMP3 and MMP13 were inhibited after the expression of PA28γ was decreased (Figures 8d, 8e, 8l, and 8m). Inflammation-related proteins (IL-1β and COX2) were increased in the DMM group, and the increases of IL-1β and COX2 were inhibited after the expression of PA28γ was decreased (Figures 8f, 8g, 8n, and 8o). ER stress-related protein (CHOP) was increased in the DMM group, and the increase of CHOP was inhibited after the expression of PA28γ was decreased (Figures 8h and 8p).

Discussion

OA is a common chronic inflammatory disease related to age, and its pathological mechanisms include local cartilage destruction, ectopic bone formation, synovitis, and systemic pathological abnormalities.[1,31-33] With the gradual increase of global population ageing, the incidence of OA is also gradually increasing, resulting in a great economic burden in terms of disease burden and disease cost.[34] Currently, there is no effective way to prevent the progression of OA, and

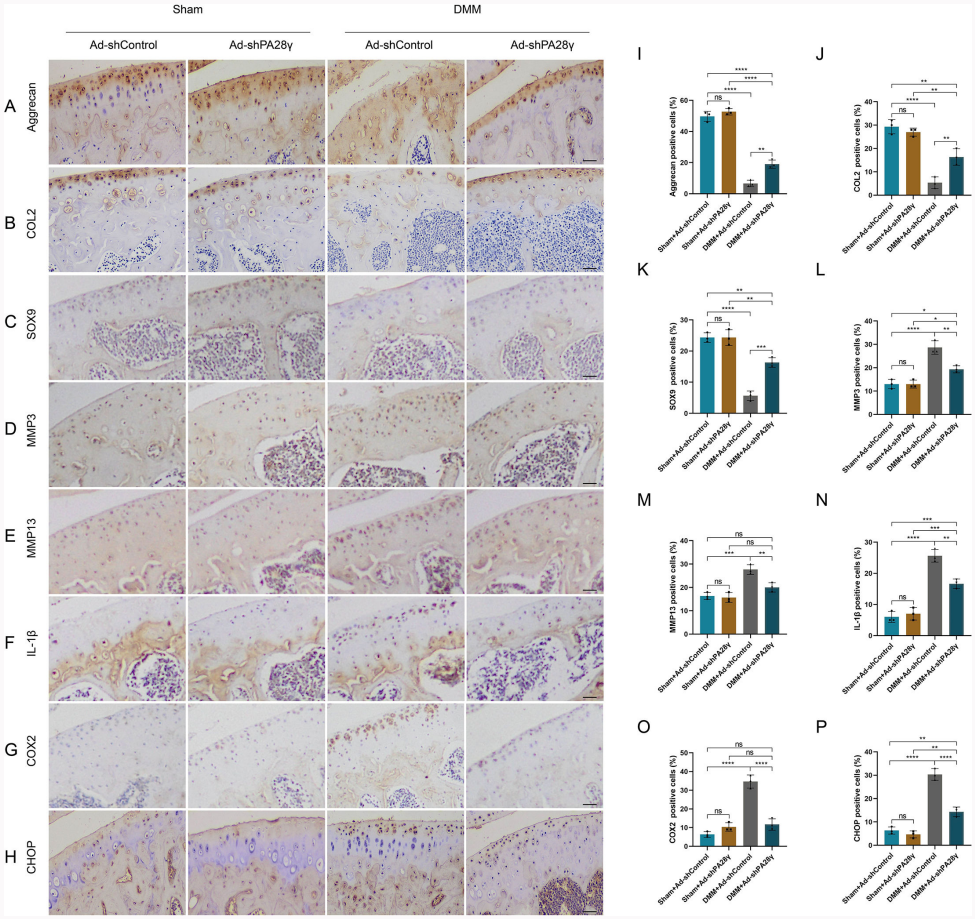

Fig. 8

Knockdown of PA28γ alleviates osteoarthritis (OA) after destabilized medial meniscus (DMM) surgery. a) and i) Aggrecan immunohistochemical staining images and quantitative data of knee joint tissue obtained from Ad-shControl and Ad-shPA28γ mice eight weeks after DMM surgery, measuring scale = 100 μm (n = 3, **p < 0.01, ****p < 0.0001). b) and j) Type II collagen (COL2) immunohistochemical staining images and quantitative data of knee joint tissue obtained from Ad shControl and Ad-shPA28γ mice eight weeks after DMM surgery, measuring scale = 100 μm (n = 3, **p < 0.01, ****p < 0.0001). c) and k) SOX9 immunohistochemical staining images and quantitative data of knee joint tissue obtained from Ad-shControl and Ad-shPA28γ mice eight weeks after DMM surgery, measuring scale = 100 μm (n = 3, **p < 0.01, ***p < 0.001, ****p < 0.0001). d) and l) Matrix metalloproteinase 3 (MMP3) immunohistochemical staining images and quantitative data of knee joint tissue obtained from Ad-shControl and Ad-shPA28γ mice eight weeks after DMM surgery, measuring scale = 100 μm (n = 3, *p < 0.05, **p < 0.01, ****p < 0.0001). e) and m) MMP13 immunohistochemical staining images and quantitative data of knee joint tissue obtained from Ad-shControl and Ad-shPA28γ mice eight weeks after DMM surgery, measuring scale = 100 μm (n = 3, **p < 0.01, ***p < 0.001). f) and n) Interleukin-1β (IL-1β) immunohistochemical staining images and quantitative data of knee joint tissue obtained from Ad-shControl and Ad-shPA28γ mice eight weeks after DMM surgery, measuring scale = 100 μm (n = 3, **p < 0.01, ***p < 0.001, ****p < 0.0001). g) and o) COX2 immunohistochemical staining images and quantitative data of knee joint tissue obtained from Ad-shControl and Ad-shPA28γ mice eight weeks after DMM surgery, measuring scale = 100 μm (n = 3, ****p < 0.0001). h) and p) CHOP immunohistochemical staining images and quantitative data of knee joint tissue obtained from Ad-shControl and Ad-shPA28γ mice eight weeks after DMM surgery, measuring scale = 100 μm (n = 3, **p < 0.01, ****p < 0.0001). ns, not specified.

joint arthroplasty is an effective treatment for end-stage OA; however, functional outcomes are not guaranteed, and the lifespan of prostheses is limited.[2] Therefore, there is an urgent need to explore the molecular mechanisms of OA pathogenesis and corresponding therapeutic targets. PA28γ has been found to promote inflammation of the colon and interstitial cells of the testis.[23,24] Therefore, we aimed to determine the association between PA28γ and OA. We found that IL-1β treatment of chondrocytes significantly induced PA28γ expression. Reducing the expression of PA28γ in chondrocytes can effectively increase the expression of proteins involved in anabolism such as COL2 and SOX9, effectively reduce the expression of proteins involved in catabolism such as MMP3 and MMP13, reduce the degradation of extracellular matrix during the development of OA, and alleviate OA effectively.

Inflammatory responses accelerate the degradation of extracellular matrix during OA development.[35-37] Our results show that IL-1β elevates inflammatory markers such as iNOS and COX2 in chondrocytes, while PA28γ knockdown partially reverses these changes. Chondrocyte apoptosis is very important in the occurrence and development of OA. Chondrocyte apoptosis depends on the phagocytosis of apoptotic bodies, resulting in a large number of apoptotic residues and secondary necrosis of the articular cartilage.[38] Cartilage cell apoptosis can destroy the structure of the articular cartilage, proteoglycan, and collagen network, thus inducing damage to the cartilage matrix, leading to serious cartilage degeneration which is accompanied by an increase in MMP-2 and MMP-3 levels, and subsequently leading to an increase in the apoptosis of chondrocytes. Thus, chondrocyte apoptosis and cartilage matrix damage form a vicious

circle.[39,40] At present, a number of studies have confirmed that many drugs can treat OA by inhibiting chondrocyte apoptosis, such as theaflavin[41] and quercetin.[42] Many genetic targets, such as BMP5[43] and SIRT3,[44] regulate OA by regulating chondrocyte apoptosis. In this study, the number of chondrocytes was reduced after IL-1β treatment, and the deletion of PA28γ partially reversed these changes. Moreover, the ratio of BAX/BCL2 and CLV Caspase3/T Caspase3 decreased after PA28γ knockout, suggesting that PA28γ can inhibit the apoptosis of chondrocytes and thus play a role in the treatment of OA.

Normally, the ER is responsible for most protein synthesis and folding within cells. In abnormal cases, ER stress is activated, and unfolded or misfolded proteins accumulate in large quantities, causing inflammation and apoptosis.[17,45,46] A large number of studies have proved that ER stress can promote the development of OA,[47-49] and the related biomarkers of ER stress, including PERK, IRE1α, GRP78, and CHOP, play an important role in OA.[50-53] Chondrocytes are the only resident cells in cartilage, and their anabolic and catabolic abnormalities can lead to the imbalance of extracellular matrix, which leads to cartilage degeneration. CHOP is an important downstream transcription factor for ER stress, and CHOP inhibits extracellular matrix production in cartilage via the AMPKα-SIRT1 pathway.[54] Meanwhile, ER stress accelerates ECM degradation in cartilage by upregulating MMP13 expression via the MAPK pathway.[55] In the occurrence and development of OA, accompanied by the production of inflammatory cytokines, these inflammatory cytokines will induce an inflammatory response, resulting in further aggravation of OA. One 2018 study found that vitexin can alleviate OA: ER stress-activated NF-κB pathway and the induced expression of inflammatory cytokines were significantly inhibited by vitexin.[51] Chondrocyte apoptosis is an important area of research when it comes to the progression of OA.[56] Inhibition of ER stress to inhibit chondrocyte apoptosis is an effective treatment for OA. Dapagliflozin (DAPA) could inhibit the PERK-eIF2α-CHOP axis of the ER stress response by activating Sirt1 in chondrocytes, preventing the apoptosis of chondrocytes and alleviating OA.[57] Melatonin could promote Sirt1 expression and inhibit IRE1α-XBP1S-CHOP to reduce ER stress-mediated apoptosis in chondrocytes and produce therapeutic effects on OA.[58] Therefore, exploring the gene targets related to ER stress is conducive to finding potential therapies for OA. In this study, we found that PA28γ knockdown in chondrocytes inhibited IL-1β or TBHP-induced ER stress and affected the phosphorylation of IRE1α and the expression of TRAF2, thereby affecting the MAPK and NF-κB signalling pathways, and finally affecting the inflammatory response of chondrocytes. Research has found that phosphorylation of STAT3 may have an important role in the inflammatory response of OA.[59] Moreover, ER stress is enhanced when the phosphorylation of STAT3 is inhibited.[60,61] Therefore, in this study, after inhibiting the expression of PA28γ in chondrocytes, we focused on the effect of STAT3 phosphorylation on ER stress in chondrocytes, which may better explore the role of STAT3 phosphorylation in the inflammatory response of OA.

The DMM mouse model, which is an established method for studying OA, can better simulate the pathophysiology process of OA and has been widely used in preclinical drug screening, evaluation, and disease pathogenesis research. In this study, significant proteoglycan loss and cartilage degeneration were observed in the DMM group, while cartilage degeneration was partially alleviated after intra-articular injection of AD-SHPA28γ in mice. Immunohistochemistry showed that anabolism was weakened, while catabolism, inflammation, and ER stress were enhanced in the cartilage of the DMM group. After intra-articular injection of AD-SHPA28γ in mice, these changes were reversed to some extent. These results suggest that reducing the expression of PA28γ in chondrocytes can delay the progression of OA in vivo.

However, this study has some limitations. First, we only studied the effect of reduced PA28γ expression on chondrocytes and OA, but did not study the related effect of increased PA28γ expression on chondrocytes and OA. Second, it would be more rigorous if chondrocyte-specific PA28γ-deficient and PA28γ-overexpressed mice could be used. We can obtain mice deficient in PA28γ and mice overexpressing PA28γ by using Cre Lox system.[62] Future studies should address these limitations.

In conclusion, our results suggest that PA28γ knockdown in chondrocytes can inhibit anabolic and catabolic dysregulation, inflammatory response, and apoptosis in OA. Moreover, PA28γ knockdown in chondrocytes can inhibit TBHP-induced ER stress by promoting STAT3 phosphorylation. These findings demonstrate that PA28γ is a potential therapeutic target for OA

Supplementary material

The original data of western blots and the no primary antibody controls of immunohistochemistry.

References

1. **Martel-Pelletier J**, **Barr AJ**, **Cicuttini FM**, **et al**. Osteoarthritis. *Nat Rev Dis Primers*. 2016;2:16072.
2. **Glyn-Jones S**, **Palmer AJR**, **Agricola R**, **et al**. Osteoarthritis. *Lancet*. 2015;386(9991):376–387.
3. **Dieppe PA**, **Lohmander LS**. Pathogenesis and management of pain in osteoarthritis. *The Lancet*. 2005;365(9463):965–973.
4. **Quicke JG**, **Conaghan PG**, **Corp N**, **Peat G**. Osteoarthritis year in review 2021: Epidemiology & therapy. *Osteoarthr Cartil*. 2022;30(2):196–206.
5. **Kraus VB**, **Blanco FJ**, **Englund M**, **Karsdal MA**, **Lohmander LS**. Call for standardized definitions of osteoarthritis and risk stratification for clinical trials and clinical use. *Osteoarthr Cartil*. 2015;23(8):1233–1241.
6. **Li K**, **Zhang Y**, **Zhang Y**, **et al**. Tyrosine kinase fyn promotes osteoarthritis by activating the β-catenin pathway. *Ann Rheum Dis*. 2018;77(6):935–943.
7. **Goldring MB**, **Goldring SR**. Osteoarthritis. *J Cell Physiol*. 2007;213(3):626–634.
8. **Chen X**, **Gong W**, **Shao X**, **et al**. METTL3-mediated m^{6}A modification of ATG7 regulates autophagy-GATA4 axis to promote cellular senescence and osteoarthritis progression. *Ann Rheum Dis*. 2022;81(1):87–99.
9. **Feng K**, **Chen Z**, **Pengcheng L**, **Zhang S**, **Wang X**. Quercetin attenuates oxidative stress-induced apoptosis via SIRT1/AMPK-mediated inhibition of ER stress in rat chondrocytes and prevents the progression of osteoarthritis in a rat model. *J Cell Physiol*. 2019;234(10):18192–18205.
10. **An S**, **Hu H**, **Li Y**, **Hu Y**. Pyroptosis plays a role in osteoarthritis. *Aging Dis*. 2020;11(5):1146–1157.
11. **Hotamisligil GS**. Endoplasmic reticulum stress and the inflammatory basis of metabolic disease. *Cell*. 2010;140(6):900–917.
12. **Tudorachi NB**, **Totu EE**, **Fifere A**, **et al**. The implication of reactive oxygen species and antioxidants in knee osteoarthritis. *Antioxidants*. 2021;10(6):985.
13. **Braakman I**, **Hebert DN**. Protein folding in the endoplasmic reticulum. *Cold Spring Harb Perspect Biol*. 2013;5(5):a013201.

14. **Reid DW**, **Nicchitta CV**. Diversity and selectivity in mRNA translation on the endoplasmic reticulum. *Nat Rev Mol Cell Biol*. 2015;16(4):221–231.
15. **Schwarz DS**, **Blower MD**. The endoplasmic reticulum: structure, function and response to cellular signaling. *Cell Mol Life Sci*. 2016;73(1): 79–94.
16. **Wang M**, **Kaufman RJ**. Protein misfolding in the endoplasmic reticulum as a conduit to human disease. *Nature*. 2016;529(7586):326–335.
17. **Hetz C**. The unfolded protein response: controlling cell fate decisions under ER stress and beyond. *Nat Rev Mol Cell Biol*. 2012;13(2):89–102.
18. **Chen J**, **Xie J-J**, **Shi K-S**, **et al**. Glucagon-like peptide-1 receptor regulates endoplasmic reticulum stress-induced apoptosis and the associated inflammatory response in chondrocytes and the progression of osteoarthritis in rat. *Cell Death Dis*. 2018;9(2):212.
19. **Zhang Z**, **Wu J**, **Teng C**, **et al**. Safranal treatment induces sirt1 expression and inhibits endoplasmic reticulum stress in mouse chondrocytes and alleviates osteoarthritis progression in a mouse model. *J Agric Food Chem*. 2022;70(31):9748–9759.
20. **Cascio P**. PA28γ: new insights on an ancient proteasome activator. *Biomolecules*. 2021;11(2):228.
21. **Magni M**, **Ruscica V**, **Buscemi G**, **et al**. Chk2 and REGγ-dependent DBC1 regulation in DNA damage induced apoptosis. *Nucleic Acids Res*. 2014;42(21):13150–13160.
22. **Jonik-Nowak B**, **Menneteau T**, **Fesquet D**, **et al**. PIP30/FAM192A is a novel regulator of the nuclear proteasome activator PA28γ. *Proc Natl Acad Sci USA*. 2018;115(28):E6477–E6486.
23. **Xu J**, **Zhou L**, **Ji L**, **et al**. The REGγ-proteasome forms a regulatory circuit with IκBε and NFκB in experimental colitis. *Nat Commun*. 2016;7:10761.
24. **Xie T**, **Chen H**, **Shen S**, **et al**. Proteasome activator REGγ promotes inflammation in leydig cells via IkBε signaling. *Int J Mol Med*. 2019;43(5): 1961–1968.
25. **You H**, **Zhang R**, **Wang L**, **Pan Q**, **Mao Z**, **Huang X**. Chondro-protective effects of shikimic acid on osteoarthritis via restoring impaired autophagy and suppressing the MAPK/NF-κB signaling pathway. *Front Pharmacol*. 2021;12:634822.
26. **Shivnath N**, **Rawat V**, **Siddiqui S**, **et al**. Antiosteoarthritic effect of Punica granatum L. peel extract on collagenase induced osteoarthritis rat by modulation of COL-2, MMP-3, and COX-2 expression. *Environ Toxicol*. 2021;36(1):5–15.
27. **Zheng W**, **Zhang H**, **Jin Y**, **et al**. Butein inhibits IL-1β-induced inflammatory response in human osteoarthritis chondrocytes and slows the progression of osteoarthritis in mice. *Int Immunopharmacol*. 2017;42: 1–10.
28. **Wang B-W**, **Jiang Y**, **Yao Z-L**, **Chen P-S**, **Yu B**, **Wang S-N**. Aucubin protects chondrocytes against IL-1β-induced apoptosis in vitro and inhibits osteoarthritis in mice model. *Drug Des Devel Ther*. 2019;13:3529–3538.
29. **Keestra-Gounder AM**, **Byndloss MX**, **Seyffert N**, **et al**. NOD1 and NOD2 signalling links ER stress with inflammation. *Nature*. 2016; 532(7599):394–397.
30. **Urano F**, **Wang X**, **Bertolotti A**, **et al**. Coupling of stress in the ER to activation of JNK protein kinases by transmembrane protein kinase IRE1. *Science*. 2000;287(5453):664–666.
31. **Abramoff B**, **Caldera FE**. Osteoarthritis: Pathology, diagnosis, and treatment options. *Med Clin North Am*. 2020;104(2):293–311.
32. **Luobu Z**, **Wang L**, **Jiang D**, **Liao T**, **Luobu C**, **Qunpei L**. CircSCAPER contributes to IL-1β-induced osteoarthritis in vitro via mir-140-3p/EZH2 axis. *Bone Joint Res*. 2022;11(2):61–72.
33. **Chen M-F**, **Hu C-C**, **Hsu Y-H**, **et al**. The role of EDIL3 in maintaining cartilage extracellular matrix and inhibiting osteoarthritis development. *Bone Joint Res*. 2023;12(12):734–746.
34. **Hiligsmann M**, **Cooper C**, **Arden N**, **et al**. Health economics in the field of osteoarthritis: An expert's consensus paper from the european society for clinical and economic aspects of osteoporosis and osteoarthritis (ESCEO). *Semin Arthritis Rheum*. 2013;43(3):303–313.
35. **Kapoor M**, **Martel-Pelletier J**, **Lajeunesse D**, **Pelletier J-P**, **Fahmi H**. Role of proinflammatory cytokines in the pathophysiology of osteoarthritis. *Nat Rev Rheumatol*. 2011;7(1):33–42.
36. **Zhou Y**, **Li J**, **Xu F**, **Ji E**, **Wang C**, **Pan Z**. Long noncoding RNA H19 alleviates inflammation in osteoarthritis through interactions between TP53, IL-38, and IL-36 receptor. *Bone Joint Res*. 2022;11(8):594–607.
37. **Lu R**, **Wang Y-G**, **Qu Y**, **et al**. Dihydrocaffeic acid improves IL-1β-induced inflammation and cartilage degradation via inhibiting NF-κB and MAPK signalling pathways. *Bone Joint Res*. 2023;12(4):259–273.
38. **Hwang HS**, **Kim HA**. Chondrocyte apoptosis in the pathogenesis of osteoarthritis. *Int J Mol Sci*. 2015;16(11):26035–26054.
39. **Kim HA**, **Suh DI**, **Song YW**. Relationship between chondrocyte apoptosis and matrix depletion in human articular cartilage. *J Rheumatol*. 2001;28(9):2038–2045.
40. **Pulai JI**, **Del Carlo M Jr**, **Loeser RF**. The alpha5beta1 integrin provides matrix survival signals for normal and osteoarthritic human articular chondrocytes in vitro. *Arthritis Rheum*. 2002;46(6):1528–1535.
41. **Xu X-X**, **Zheng G**, **Tang S-K**, **Liu H-X**, **Hu Y-Z**, **Shang P**. Theaflavin protects chondrocytes against apoptosis and senescence via regulating nrf2 and ameliorates murine osteoarthritis. *Food Funct*. 2021;12(4):1590–1602.
42. **Li W**, **Wang Y**, **Tang Y**, **et al**. Quercetin alleviates osteoarthritis progression in rats by suppressing inflammation and apoptosis via inhibition of IRAK1/NLRP3 signaling. *J Inflamm Res*. 2021;14:3393–3403.
43. **Shao Y**, **Zhao C**, **Pan J**, **et al**. BMP5 silencing inhibits chondrocyte senescence and apoptosis as well as osteoarthritis progression in mice. *Aging*. 2021;13(7):9646–9664.
44. **Xu K**, **He Y**, **Moqbel SAA**, **Zhou X**, **Wu L**, **Bao J**. SIRT3 ameliorates osteoarthritis via regulating chondrocyte autophagy and apoptosis through the PI3K/Akt/mTOR pathway. *Int J Biol Macromol*. 2021;175:351–360.
45. **Zhang K**, **Kaufman RJ**. From endoplasmic-reticulum stress to the inflammatory response. *Nature*. 2008;454(7203):455–462.
46. **Gorman AM**, **Healy SJM**, **Jäger R**, **Samali A**. Stress management at the ER: regulators of ER stress-induced apoptosis. *Pharmacol Ther*. 2012; 134(3):306–316.
47. **Zhu Z**, **Gao S**, **Chen C**, **et al**. The natural product salicin alleviates osteoarthritis progression by binding to IRE1α and inhibiting endoplasmic reticulum stress through the IRE1α-IκBα-p65 signaling pathway. *Exp Mol Med*. 2022;54(11):1927–1939.
48. **Guo F-J**, **Xiong Z**, **Lu X**, **Ye M**, **Han X**, **Jiang R**. ATF6 upregulates XBP1S and inhibits ER stress-mediated apoptosis in osteoarthritis cartilage. *Cell Signal*. 2014;26(2):332–342.
49. **Wang Y**, **Fan A**, **Lu L**, **et al**. Exosome modification to better alleviates endoplasmic reticulum stress induced chondrocyte apoptosis and osteoarthritis. *Biochem Pharmacol*. 2022;206:115343.
50. **Puthalakath H**, **O'Reilly LA**, **Gunn P**, **et al**. ER stress triggers apoptosis by activating BH3-only protein Bim. *Cell*. 2007;129(7):1337–1349.
51. **Xie C-L**, **Li J-L**, **Xue E-X**, **et al**. Vitexin alleviates ER-stress-activated apoptosis and the related inflammation in chondrocytes and inhibits the degeneration of cartilage in rats. *Food Funct*. 2018;9(11):5740–5749.
52. **Li Y-H**, **Tardif G**, **Hum D**, **et al**. The unfolded protein response genes in human osteoarthritic chondrocytes: PERK emerges as a potential therapeutic target. *Arthritis Res Ther*. 2016;18(1):172.
53. **Haywood J**, **Yammani RR**. Free fatty acid palmitate activates unfolded protein response pathway and promotes apoptosis in meniscus cells. *Osteoarthr Cartil*. 2016;24(5):942–945.
54. **Yu X**, **Xu X**, **Dong W**, **et al**. DDIT3/CHOP mediates the inhibitory effect of ER stress on chondrocyte differentiation by AMPKα-SIRT1 pathway. *Biochim Biophys Acta Mol Cell Res*. 2022;1869(8):119265.
55. **Hamamura K**, **Goldring MB**, **Yokota H**. Involvement of p38 MAPK in regulation of MMP13 mRNA in chondrocytes in response to surviving stress to endoplasmic reticulum. *Arch Oral Biol*. 2009;54(3):279–286.
56. **Uehara Y**, **Hirose J**, **Yamabe S**, **et al**. Endoplasmic reticulum stress-induced apoptosis contributes to articular cartilage degeneration via C/EBP homologous protein. *Osteoarthr Cartil*. 2014;22(7):1007–1017.
57. **Liu Z**, **Huang J**, **Wang X**, **et al**. Dapagliflozin suppress endoplasmic reticulum stress mediated apoptosis of chondrocytes by activating Sirt1. *Chem Biol Interact*. 2023;384:110724.
58. **Qin K**, **Tang H**, **Ren Y**, **et al**. Melatonin promotes sirtuin 1 expression and inhibits IRE1α–XBP1S–CHOP to reduce endoplasmic reticulum stress–mediated apoptosis in chondrocytes. *Front Pharmacol*. 2022; 13:940629.
59. **Chen B**, **Ning K**, **Sun M-L**, **Zhang X-A**. Regulation and therapy, the role of JAK2/STAT3 signaling pathway in OA: a systematic review. *Cell Commun Signal*. 2023;21(1):67.
60. **Song M**, **Wang C**, **Yang H**, **et al**. P-STAT3 inhibition activates endoplasmic reticulum stress-induced splenocyte apoptosis in chronic stress. *Front Physiol*. 2020;11:680.
61. **Zhang X**, **Zhang S**, **Sun Q**, **Jiao W**, **Yan Y**, **Zhang X**. Compound K induces endoplasmic reticulum stress and apoptosis in human liver cancer cells by regulating STAT3. *Molecules*. 2018;23(6):1482.

62. **Tu J**, **Zhang H**, **Yang T**, **et al**. Aging-associated REGγ proteasome decline predisposes to tauopathy. *J Biol Chem*. 2022;298(11):102571.

Author information

H. Mo, PhD, Researcher
K. Sun, PhD, Researcher
Y. Hou, MMed, Researcher
Z. Ruan, MMed, Researcher
Z. He, MD, Researcher
H. Liu, PhD, Researcher
Z. Wang, PhD, Researcher
F. Guo, PhD, Researcher
Department of Orthopedics, Tongji Hospital, Tongji Medical College, Huazhong University of Science and Technology, Wuhan, China.

L. Li, PhD, Researcher, Department of Orthopedics, Tongji Hospital, Tongji Medical College, Huazhong University of Science and Technology, Wuhan, China; Wuhan National High Magnetic Field Center, Huazhong University of Science and Technology, Wuhan, China.

Author contributions

H. Mo: Conceptualization, Data curation, Investigation, Writing – original draft, Formal analysis.
K. Sun: Investigation, Methodology.
Y. Hou: Investigation, Writing – original draft.
Z. Ruan: Validation, Visualization.
Z. He: Investigation.
H. Liu: Investigation.
L. Li: Investigation, Validation, Visualization, Project administration.
Z. Wang: Data curation, Investigation, Methodology, Writing – review & editing.
F. Guo: Investigation, Methodology, Project administration, Writing – review & editing.

Z. Wang and F. Guo contributed equally to this work.

Z. Wang and F. Guo are joint senior authors.

Funding statement

The authors disclose receipt of the following financial or material support for the research, authorship, and/or publication of this article: this work was supported by instiutional funding as awarded by the National Natural Science Foundation of China (No. 82172498).

ICMJE COI statement

This work was supported by institutional funding as awarded by the National Natural Science Foundation of China (No. 82172498).

Data sharing

The data that support the findings for this study are available to other researchers from the corresponding author upon reasonable request.

Acknowledgements

The authors wish to thank the National Natural Science Foundation of China for funding assistance with this research.

Ethical review statement

The animal study was reviewed and approved by the Animal Care and Use Committee for Teaching and Research, Tongji Medical College, Huazhong University of Science and Technology (IACUC Number: 2685).

Open access funding

The authors report that they received open access funding for their manuscript from the National Natural Science Foundation of China (No. 82172498)